

This article was downloaded by:

On: 22 January 2011

Access details: *Access Details: Free Access*

Publisher *Taylor & Francis*

Informa Ltd Registered in England and Wales Registered Number: 1072954 Registered office: Mortimer House, 37-41 Mortimer Street, London W1T 3JH, UK



The Journal of Adhesion

Publication details, including instructions for authors and subscription information:

<http://www.informaworld.com/smpp/title~content=t713453635>

An Ultrasonic Evaluation and Quality Control Tool for Adhesive Bonds

Graham H. Thomas; Joseph L. Rose

To cite this Article Thomas, Graham H. and Rose, Joseph L.(1980) 'An Ultrasonic Evaluation and Quality Control Tool for Adhesive Bonds', *The Journal of Adhesion*, 10: 4, 293 – 316

To link to this Article: DOI: 10.1080/0021846808544635

URL: <http://dx.doi.org/10.1080/0021846808544635>

PLEASE SCROLL DOWN FOR ARTICLE

Full terms and conditions of use: <http://www.informaworld.com/terms-and-conditions-of-access.pdf>

This article may be used for research, teaching and private study purposes. Any substantial or systematic reproduction, re-distribution, re-selling, loan or sub-licensing, systematic supply or distribution in any form to anyone is expressly forbidden.

The publisher does not give any warranty express or implied or make any representation that the contents will be complete or accurate or up to date. The accuracy of any instructions, formulae and drug doses should be independently verified with primary sources. The publisher shall not be liable for any loss, actions, claims, proceedings, demand or costs or damages whatsoever or howsoever caused arising directly or indirectly in connection with or arising out of the use of this material.

An Ultrasonic Evaluation and Quality Control Tool for Adhesive Bonds

GRAHAM H. THOMAS†

Member of the Technical Staff, Sandia Laboratories Livermore, CA 94550, U.S.A.

JOSEPH L. ROSE

Professor of Mechanical Engineering, Drexel University, Philadelphia, PA 19104, U.S.A.

(Received June 1, 1979; in final form December 3, 1979)

The problem of predicting adhesive bond performance for both surface preparation and undercure defects has been studied using an ultrasonic, experimental test bed system. This experimental test bed incorporates the ultrasonic and computer equipment necessary to acquire and process data from various types of adhesively bonded test specimens. The computer hardware and software has been developed to allow the design of reliable pattern recognition algorithms for the evaluation of surface preparation and bond cure. The specific problem studied is the inspection of the adhesive bond in an aluminum to aluminum step-lap joint whose strength could be affected by improper surface preparation or undercure. A set of 154 bond specimens was used to design an algorithm that is 91% reliable for separating the specimens into a good class, those bonds with no defects, or a weak class, bonds with poor surface preparation or undercured adhesive layer. A Fisher Linear Discriminant function was selected by the test bed as the best pattern recognition routine for this classification problem.

INTRODUCTION

Adhesive bonding is rapidly becoming an important part of joint technology because of its inherent nature to provide more uniform stress transfer, increased fatigue life, and a reduction in structural weight. These characteristics are particularly important in high performance structures utilizing

† Formerly a Graduate Student at Drexel University.

aluminum-to-aluminum and aluminum-to-composite joints such as those found in aircraft. Adhesives are often suitable for solving many joining problems compared to the more common techniques of welding, riveting, and the use of other mechanical fasteners. One of the major limitations on the use of adhesives as a structural element, however, is associated with the difficulty encountered in making an accurate determination of bond quality or potential performance after the joint has been completely assembled. An important part of using adhesives is to develop a nondestructive evaluation technique that makes use of a single ultrasonic measurement for predicting the potential bond performance level.

Recently many investigators have studied this difficult problem of ultrasonic inspection of adhesive joints. The more successful techniques for determining bond strength where gross flaws are not present have been with the aid of computerized, sophisticated signal processing and feature extraction. Rose and Raisch¹ used a theoretical modeling approach to determine significant features for their prediction of adhesively defective bonds. Their procedure incorporated an automatic scanning, fast data acquisition system, and a fuzzy logic pattern recognition algorithm to classify bond specimens as either good or bad with 87% reliability. P. L. Flynn² has attacked the cohesive failure prediction problem in much the same way. Chang *et al.*³ used combinations of features from the amplitude-time and amplitude-frequency domains to classify adhesive bonds into groups of properly prepared and improperly prepared substrates after the bond was assembled. Couchman *et al.*⁴ have developed a decision algorithm for predicting adhesive bond strength that evolved from a study done by Chang *et al.*,³ and could be adapted to a bond strength prediction meter for on site bond inspections. Alers *et al.*^{5,6} have used theoretical modeling to generate ultrasonic echoes for a variety of types of defective bonds. Mucciardi and Elsley⁷ have instituted adaptive learning network techniques to classify bond strength and have been 80% reliable in separating good bonds from those with porosity, voids or delaminations. And finally, as the predecessor to this paper, Rose and Thomas⁸ have incorporated a computer automated test bed system, an advanced Fisher Linear Discriminant pattern recognition algorithm and deconvolution techniques to predict adhesive defects of bonded step-lap joints in aluminum to aluminum with 92% reliability. The deconvolution algorithm, as described by Rose and Avoili,⁹ was incorporated in Rose and Thomas' algorithm to provide transducer compensation necessary to the usefulness of such a bond strength prediction scheme.

Though a tremendous advance in the state of the art of ultrasonic adhesive bond inspection has been made, there still exists much work to be done in the area of producing a complete bond flaw prediction algorithm which includes all bonding defects. The solution to this problem is the goal of this

study. The problem of developing a complete bond flaw prediction algorithm has been attacked by assembling an ultrasonic design tool and experimental test bed for the prediction of adhesive bond defects. This system includes ultrasonic equipment, computer hardware, and software for the design of adhesive bond defect prediction algorithms which could account for a variety of bonding flaws. A sample adhesive bonding problem has been studied using this test bed system.

TEST BED CONCEPT

The test bed idea was conceptualized out of need for a means to study new ultrasonic inspection problems that could not be solved using traditional techniques. These inspection problems required advanced, state of the art methods for solution. A test bed is a self-contained assemblage of equipment, controlled by a computer, to acquire data, process the data and design classification schemes for new ultrasonic inspection problems.

The test bed system provides a systematic approach to a new problem in ultrasonic nondestructive evaluation. Once a new inspection problem has been defined, the ultrasonic test bed can be implemented. For example, in the case of an adhesive bond problem, the first step is to perform a parametric study using Brekovskikh's layered media program¹² to model the bond structure. This study will provide a resource base for selecting pertinent features, plus determine a transducer selection criteria. The test bed equipment is then used to acquire data using the appropriate transducer from a set of training specimens. This data can next be reduced by signal processing to provide the desired feature values. After the training set's feature vectors have been determined, a collection of computer augmented pattern recognition algorithms that are included in a package called "Generalized Approach to New Problems in Ultrasonic Inspection" (GANPUI),¹⁰ can be instituted to find the optimal classification technique. A "GANPUI" flow chart is illustrated in Figure 1. This flow chart describes a logical sequence of steps starting with optimal ultrasonic signals (called clever data), extracting discriminating features from the signals, using these features to develop a pattern recognition algorithm and finally classifying the ultrasonic reflector. Once a classification algorithm has been designed, then a different set of specimens, a test set, is inspected by the test bed system and classified by the newly designed bond defect prediction algorithm to determine the algorithm's reliability. If the reliability is not adequate, the process is started from the beginning using new data acquisition techniques, selecting different features, and instituting other pattern recognition algorithms.

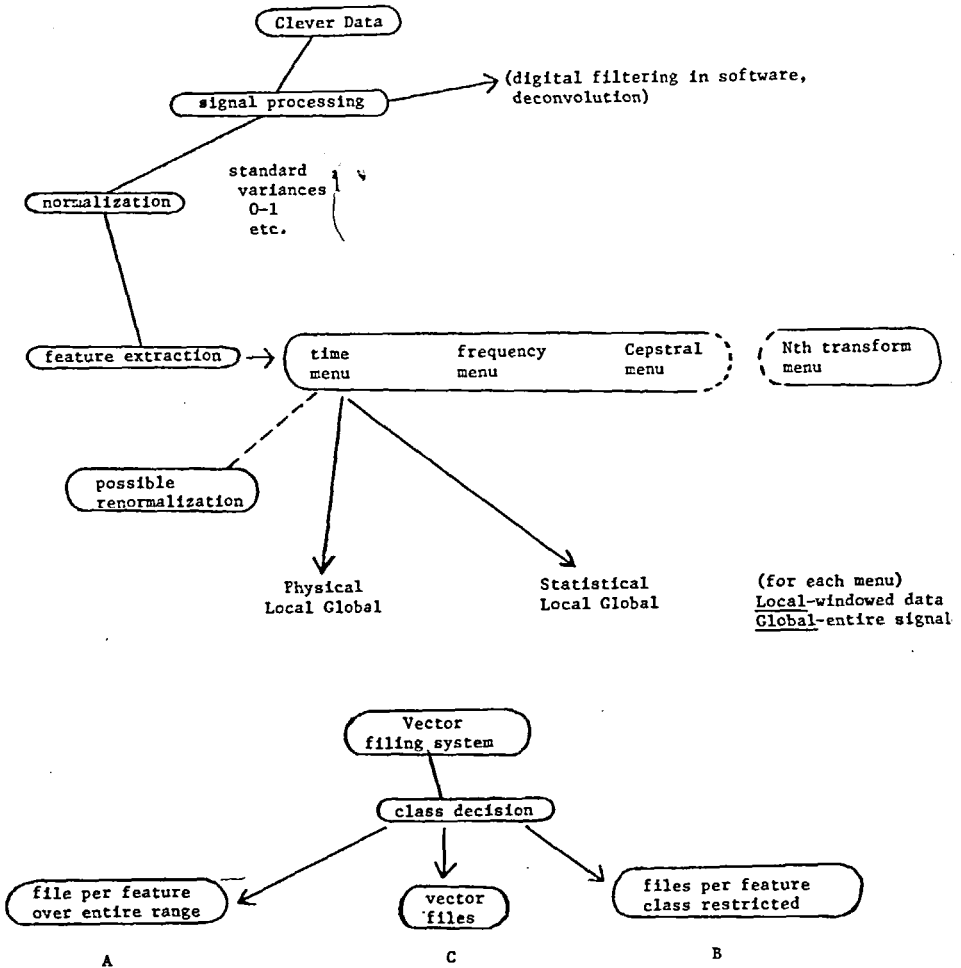


FIGURE 1 Generalized approach to new problems in ultrasonic inspection (1st page).

TEST SPECIMEN DESCRIPTION

Two series of test specimens have been fabricated for this sample study. The first series of bond specimens was used as a training set to design the bond defect prediction algorithm. This first series included good specimens, adhesively defective specimens, and cohesively defective specimens, see Table I. The second series was used to test the algorithm and it included good specimens, adhesively defective specimens, and cohesively defective specimens, see Table II. The specimen geometry is that of a typical step-lap joint

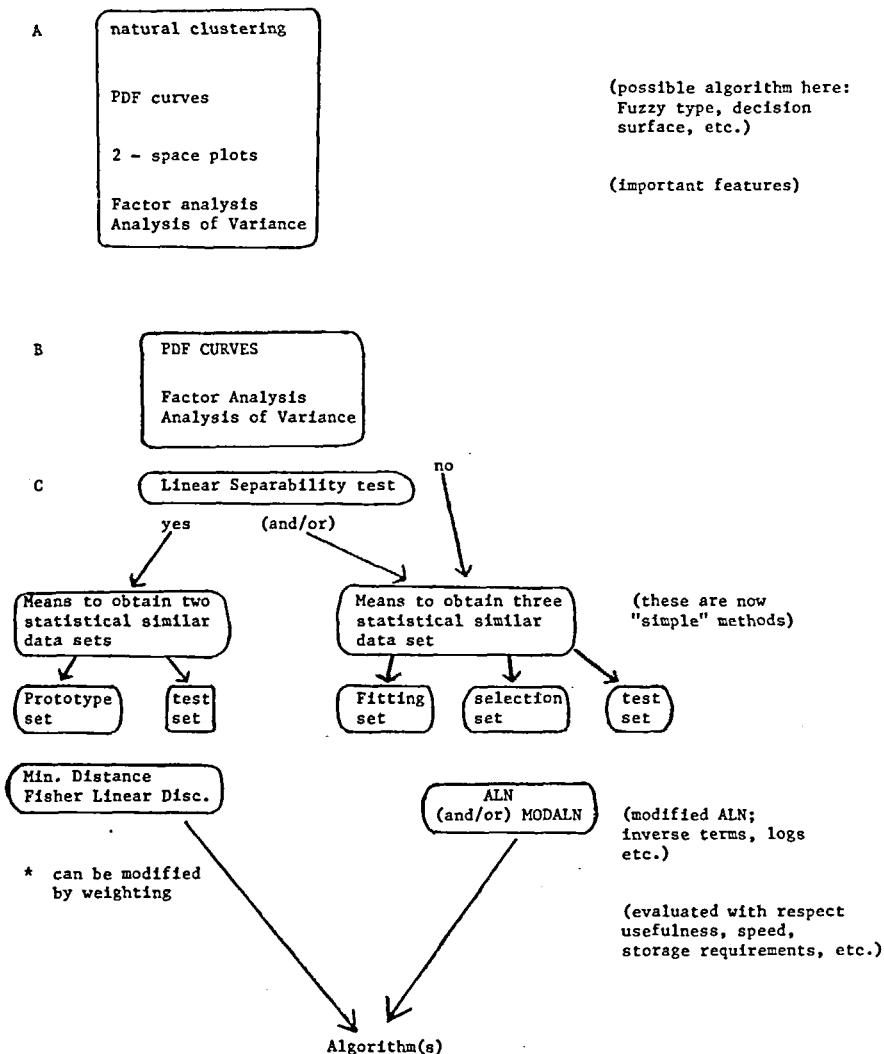


FIGURE 1 Generalized approach to new problems in ultrasonic inspection (2nd page).

as shown in Figure 2. An industrial adhesive, FM-73, from American Cyanamid Co., was used in this study. Manufacturing techniques for the adhesive system are described in the following paragraphs.

Each substrate was machined from aluminum bar stock so that its finished dimensions were $6 \times 1 \times \frac{1}{2}$ inch. A hole was drilled in the end of each half opposite the joint for mounting in an Instron testing machine for tensile strength evaluation. A 1-inch long step was cut into the other end providing a

TABLE I
Training set specimens

Specimen number	Failure load(lb.)	Programmed defect	Specimen number	Failure load(lb.)	Programmed defect
1	4420	None	32	2690	Adhesive
2	4420	None	33	2590	Adhesive
3	4420	None	34	2590	Adhesive
4	4420	None	35	2590	Adhesive
5	4340	None	36	2590	Adhesive
6	4340	None	37	2500	Adhesive
7	4340	None	38	2500	Adhesive
8	4340	None	39	2500	Adhesive
9	4290	None	40	2500	Adhesive
10	4290	None	41	2450	Adhesive
11	4290	None	42	2450	Adhesive
12	4290	None	43	2450	Adhesive
13	4250	None	44	2450	Adhesive
14	4250	None	45	1400	Adhesive
15	4250	None	46	1400	Adhesive
16	4250	None	47	1400	Adhesive
17	4150	None	48	1400	Adhesive
18	4150	None	49	770	Cohesive
19	4150	None	50	770	Cohesive
20	4150	None	52	770	Cohesive
21	3500	None	53	750	Cohesive
22	3500	None	54	750	Cohesive
23	3500	None	55	750	Cohesive
24	3500	None	56	750	Cohesive
25	2750	Adhesive	57	750	Cohesive
26	2750	Adhesive	58	750	Cohesive
27	2750	Adhesive	60	750	Cohesive
28	2750	Adhesive	61	700	Cohesive
29	2690	Adhesive	62	700	Cohesive
30	2690	Adhesive	63	700	Cohesive
31	2690	Adhesive	64	700	Cohesive

total bond area of one square inch with a nominal bond thickness of 0.005 inch (see Figure 2).

Surface preparation of the adherends is the first step in adhesive bonding. It is important to clean thoroughly all surfaces which will be in contact with the adhesive. To accomplish this, the following procedure was implemented:

- 1) The aluminum specimens were wiped free of grease, oil, and dirt with acetone and then rinsed with tap water.
- 2) A test for water break was done at this point to determine surface contamination. The water usually beaded at this time, indicating need for further cleaning.
- 3) Specimens to be etched were then immersed in a chromic-sulfuric solution for ten minutes.

TABLE II
Test set specimens

Specimen number	Failure load(lb.)	Programmed defect	Specimen number	Failure load(lb.)	Programmed defect
65	4200	None	93	690	Cohesive
66	4200	None	94	690	Cohesive
67	4200	None	95	690	Cohesive
68	4200	None	96	690	Cohesive
69	4150	None	131	510	Adhesive
70	4150	None	132	510	Adhesive
71	3900	None	133	510	Adhesive
72	3900	None	134	510	Adhesive
73	3900	None	135	500	Cohesive
74	3900	None	136	500	Cohesive
75	3730	None	137	500	Cohesive
76	3730	None	138	500	Cohesive
77	3730	None	139	490	Adhesive
78	3730	None	140	490	Adhesive
79	3450	Cohesive	141	490	Adhesive
80	3450	Cohesive	142	490	Adhesive
81	3450	Cohesive	143	470	Adhesive
82	3450	Cohesive	144	470	Adhesive
83	3400	Cohesive	145	470	Adhesive
84	3400	Cohesive	146	470	Adhesive
85	3400	Cohesive	147	470	Cohesive
86	3400	Cohesive	148	470	Cohesive
87	710	Cohesive	149	470	Cohesive
88	710	Cohesive	150	470	Cohesive
89	710	Cohesive	151	400	Adhesive
90	710	Cohesive	152	400	Adhesive
91	690	Cohesive	153	400	Adhesive
92	690	Cohesive	154	400	Adhesive

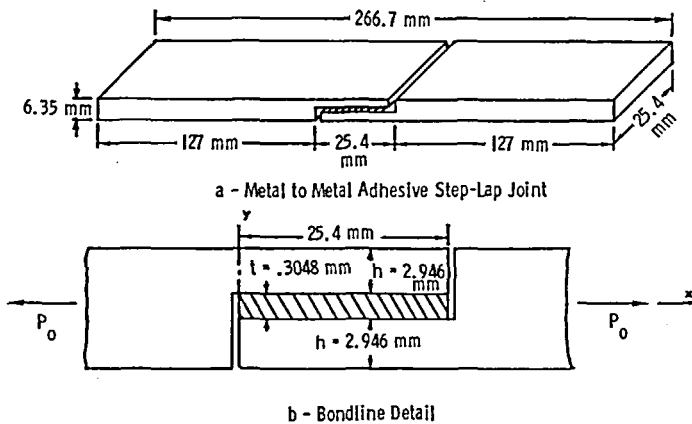


FIGURE 2 Step-lap joint test specimen (SI conversion: 25.4 mm = 1 in).

4) After 10 minutes, the etched specimens were rinsed in cold tap water and soaked in cold de-ionized water for 5 minutes. During this step, the water break test showed a smooth continuous sheet of water over the etched areas.

5) Upon removal from the de-ionized water, the specimens were dried in a vented oven at 145°F. This cleaning procedure was eliminated from the specimens that were to fail adhesively.

After the specimens had dried, they were removed from the oven and allowed to cool to room temperature. After cooling, a thin layer of primer was sprayed on the specimen surfaces which were to be in contact with the adhesive. The primer was first dried at room temperature for 30 minutes and then cured in the vented oven at 250°F for 30 minutes.

The actual bonding of the two aluminum half specimens was done in an autoclave. FM-73 adhesive is manufactured in large sheets with a skrim. The sheets may be cut to the appropriate size and shape, which in this case were 1 inch squares. The adhesive squares were placed on the bonding surfaces and the specimens placed in a jig for curing. The specimens were then sealed in an acetate bag, placed in the autoclave, and attached to a vacuum line. A vacuum of 28 to 29 inches mercury was drawn on the bag as the temperature was increased. The specimens were heated to 250°F within 30 minutes in the autoclave. The vacuum was drawn and the autoclave pressure applied until the effective bonding pressure was 40 ± 5 psi. The specimens were held at 250°F for 60 minutes and then allowed to cool to 100°F under pressure before they were removed from the autoclave.

After the specimens were removed from the jig, they were waterproofed by coating the bondline edges with polyurethane. This waterproofing was applied to eliminate the possibility of water affecting the bond during ultrasonic inspection in an immersion tank.

Several types of bonding defects were manufactured into the bond specimens so that a bond defect prediction algorithm could be developed that considered adhesive and cohesive defects. First, properly prepared and cured specimens were made to provide data from good bonds. Then, weak bonds were manufactured by either contaminating the adherent surfaces to cause an adhesive defect or under-curing the specimen to cause a cohesive failure. A list of the types of bonds used in the development and testing of the bond strength prediction algorithm is presented in Tables I and II.

DESTRUCTIVE TEST SYSTEM

After completing the ultrasonic test sequence, the bond specimen was destructively tested on an Instron Model 1230 tensile testing machine. The

specimens were held with pin grips through the holes in each end and loaded in tension until failure. The strain rate was held constant at 0.01 inches per minute. Load versus displacement was recorded on an x-y plotter for each specimen and the maximum load was noted. The weak specimens typically failed in the 500 to 2500 pound range, while the strongest specimens withstood upwards of 5000 pounds. See Table I and II. The destructive test of the adhesively bonded specimens confirmed the programming of defects in the bond layer.

ULTRASONIC TEST EQUIPMENT

An ultrasonic pulse-echo immersion system was used for the data acquisition procedures required in this experimental test bed. A block diagram of the ultrasonic equipment is shown in Figure 3. The system consists of an Aerotech UTA 2 Pulser/Receiver driving the ultrasonic inspection probe. This pulser/receiver also amplifies the returning ultrasonic RF signal and has a gate circuit to separate and output any specific part of the ultrasonic waveform. The gate signal was used in this test bed as a means to trigger the analog-to-digital converter.

A Tektronix 7704 oscilloscope was used to display the ultrasonic RF waveform along with the gate signal. This oscilloscope display was needed to align the search probe and adjust the pulser settings for optimal ultrasonic response of the probe. The oscilloscope was used in a dual trace mode, one trace for the ultrasonic RF waveform and the other for the gate. The gate display was useful for setting the trigger delay on the Biomation 8100 analog-to-digital converter. A second oscilloscope was also used in this experimental test bed. This oscilloscope's function was to monitor the memory of the analog to digital converter. Once the ultrasonic waveform was digitized and stored in the A/D converter, the converter also converts the digital information back into analog again, and this RF signal was then displayed on a monitoring oscilloscope. Thus, the second oscilloscope provided a check on the A/D converter and the signal it was digitizing.

A computer controlled x-y scanner was incorporated into this test bed system as a tool to acquire automatically and accurately ultrasonic data for a variety of bond specimen configurations. The x-y scanner, as shown in Figure 3 was attached to the top of an immersion tank in which the bond specimen was placed. The scanner included two stepper motors which drive precision threaded bars and locate the transducer to within a thousandth of an inch. The computer can control the rotation of the stepper motors and thus the location of the probe. A manual override was also used to facilitate initial location of the transducer. The transducer was attached to the scanner

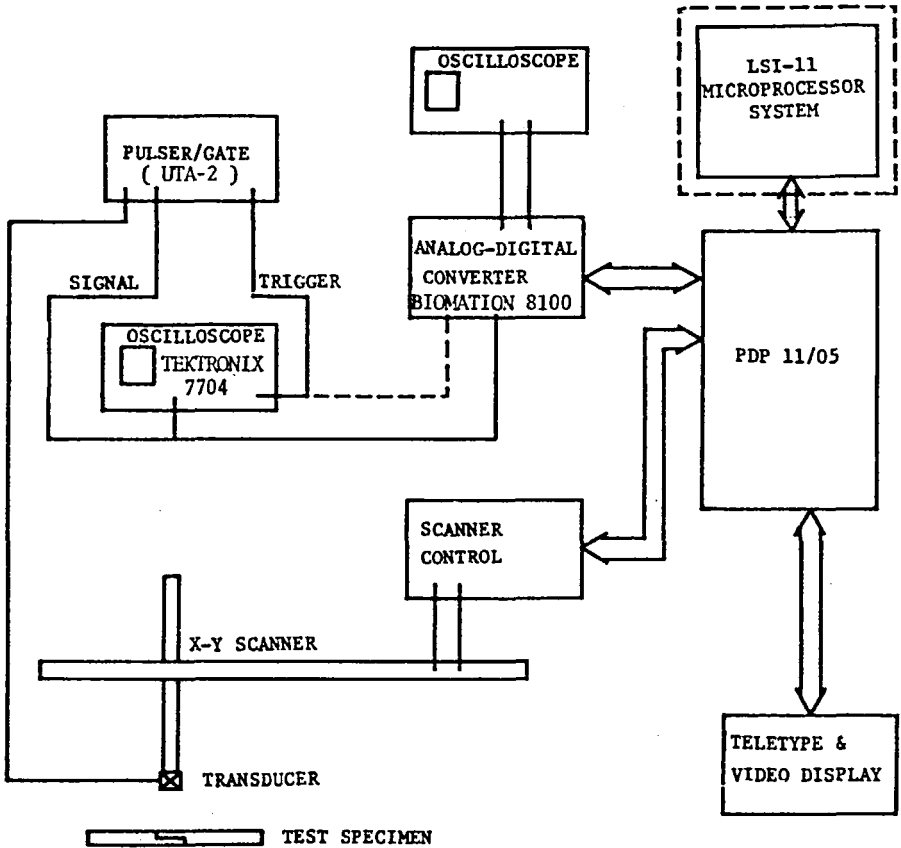


FIGURE 3 Block diagram of the fast ultrasonic data acquisition and analysis system.

by a down-tube and could be located a variable distance above the test specimen by loosening the clamp holding the down-tube and sliding the tube up or down. A standard two-axis adjustable gimbling fixture held the transducer to the down-tube. This was needed to align the transducer above the specimen.

TRANSDUCER PARAMETERS FOR ADHESIVE BOND INSPECTION

The selection of the ultrasonic probe to be used for the inspection of the adhesive bond structure is a critical phase in the assembly of the ultrasonic equipment. The transducer must convert an electrical voltage to mechanical,

sonic energy by way of the piezoelectric effect. The piezoelectric effect is a phenomenon that certain materials and natural crystals exhibit when they are exposed to an electrical voltage. The electrical voltage causes the crystal to expand and contract at a natural frequency for the specific piezoelectric element's geometry. Thus the piezoelectric material can transmit mechanical energy when it is in physical contact with another material. The piezoelectric effect also acts in the reverse manner. If the piezoelectric substance is mechanically deformed, an electrical voltage will be produced in proportion to the amount of deformation. Thus the crystal in the transducer, as well as the structure of the transducer, affects its performance. Such parameters as frequency, bandwidth, focusing, wave propagation mode, and test configuration were considered for selecting the optimal transducer. In this experimental test bed, the inspection procedures were immersion and normal beam interrogation. The other parameters, frequency content and focusing, needed more consideration before final selection. Focusing the acoustic energy of the transducer on the bond layer provided a better description of a specific point in the bonded structure; whereas a non-focused probe tended to average a larger area for that single location. Both focused and non-focused transducers were considered in this study, but the focused transducer provided a better description of the bonded structure, since a spatial averaging technique was incorporated to account for the shear stress distribution in the bond samples. The focused transducer also transmitted more acoustic energy to the area of the bond layer being inspected. Care must be taken, though, to assure that the transducer is correctly located with respect to the bond specimen so the ultrasonic energy is in fact focused on the bond line.

The main concern when selecting the inspecting transducer was to provide the proper frequency content for accurate feature value selection. A theoretical modelling approach to the adhesive bond system was conducted on a computer to determine the significant features of the ultrasonic signal which was reflected by the bond layer. Once the features were selected, a transducer acceptance criteria was established to ensure visibility of the features chosen. For example, if discriminating features were determined to occur at five and twelve megahertz, then the search probe must have a frequency bandwidth which includes these frequency modes to be acceptable.

COMPUTER HARDWARE

The automatic data acquisition system for adhesive bond inspection was developed around a Digital Equipment Corporation PDP 11/05 minicomputer with 32K core memory. As shown in Figure 4, the PDP 11/05 minicomputer also included various interface cards to accept information

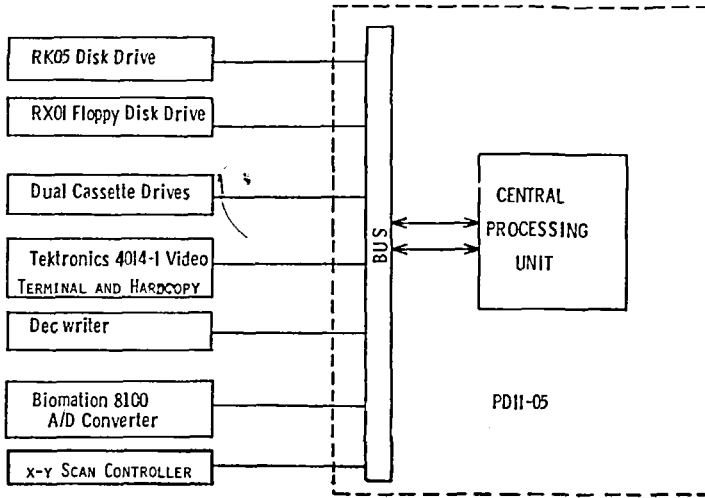


FIGURE 4 Block diagram of PD11-05 computer and peripheral equipment.

from numerous peripheral devices. Peripherals included a RK05 disk drive, RX01 floppy disk drive, dual cassette drives, Decwriter teletype and line printer, and Tektronix 4014 video terminal and 4631 hard copy unit. The RK05 hard disk was used to store the operating system for the computer and all software packages required for operation of the test bed equipment. The floppy disks and cassettes were used primarily for data storage and software back-up. The Tektronix 4014 video terminal with hard copy unit was the main peripheral for software development and graphics displays. A Decwriter was used as a back-up device to the Tektronix video terminal.

ANALOG TO DIGITAL CONVERTER

The analog-to-digital converter used in this test was a Biomation 8100 unit capable of sampling intervals to $0.01 \mu\text{sec}$. Digitizing ultrasonic RF waveforms at this rate will yield approximately ten points per cycle on a ten megahertz pulse. The converter is an eight bit machine and thus can digitize to an accuracy of one part in 256, and can store 2,048 amplitude-time points in its memory at one time. Thus, at the quickest sampling rate ($0.01 \mu\text{sec}$.) the analog to digital converter will store $20.48 \mu\text{sec}$. of data. The A/D converter can also transform the digitized signal back into analog form which may be displayed on an oscilloscope. The Biomation 8100 has been interfaced to the minicomputer through a DR11-C general input/output board. Once the digitized data has been accepted by the computer, various signal processing

techniques and graphics routines were used to enhance and display the ultrasonic waveform.

DATA ACQUISITION DETAILS

The data acquisition procedure used for ultrasonically inspecting the adhesive bond specimens is as follows: the transducer was automatically located over each of six inspection points on the bonded specimen as shown in Figure 5, and these signals were spatially weighted and averaged to account

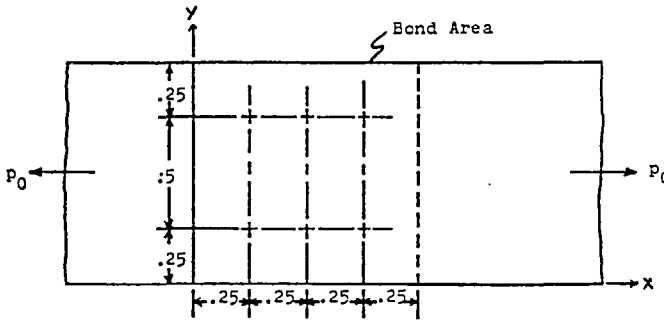


FIGURE 5 Spatial location of adhesive bond data acquisition points.

for the shear stress distribution in the step-lap joint as illustrated in Figure 6.¹¹ A one-and-a-quarter-inch water path separated the transducer from the specimen. At each location, five amplitude-time signals were averaged to eliminate some of the random noise generated by the system. Each amplitude-time signal was composed of a water-aluminum interface echo used for a reference and bond line echo made from the superposition of the aluminum-adhesive and the adhesive-aluminum interface reflections. The result of the averaging was a single reference and bond line echo which was stored in the computer's memory. A program was then called which calculates the Fourier Transforms of the reference and bond line echoes. The reference spectrum was divided, point by point, into the bond layer's echo spectrum using a complex division algorithm. This division resulted in the transfer function for the bond layer.⁹ The transfer function was then used to determine various feature values because the transfer function is a function solely of the bond layer and is independent of the transducer.

SIGNAL PROCESSING

An important phase in the development or implementation of an adhesive bond prediction algorithm is signal processing and data reduction. This is

Aluminum: $E = 10^7$ psi
 $\nu = 0.3$

Epoxy: $E = 4.45 \times 10^5$ psi
 $G = 1.65 \times 10^5$ psi

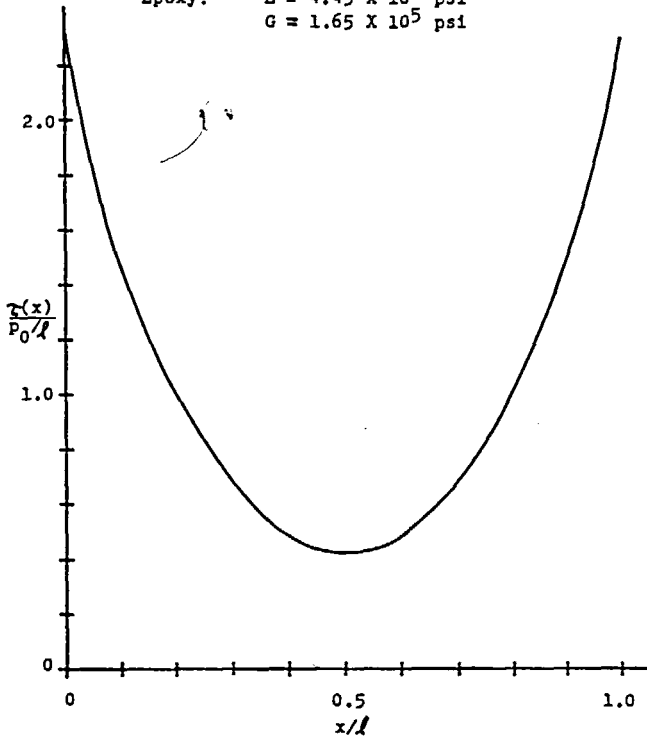


FIGURE 6 Shear stress in an aluminum-aluminum step-lap joint (1 psi = 6.8 kN/m²).

done before the feature values are determined to provide better, more accurate values. There were several noise influences in this experimental test bed system. As shown in Figure 7, noise could be added to the ultrasonic signal by various sources. One source was noise picked up by the transducer from the specimen and its surroundings. Another source of noise was from the measurement equipment. And finally, there was the quantization noise caused by the finite quantization levels of the A/D converter. Random noise was significantly reduced by averaging the ultrasonic RF waveform many times as it was passed to the computer. A moving average was rather beneficial in reducing high frequency noise by smoothing the ultrasonic signal's wave form.

The major data reduction technique used in this test bed is a Fourier Transform of the ultrasonic RF signals. The Fourier Transform allows the amplitude-time signals to be described by their frequency content. The

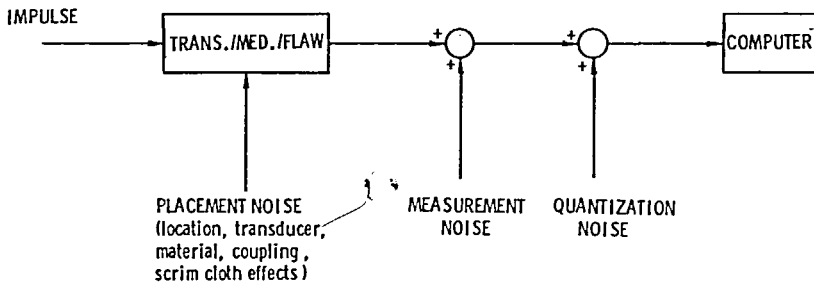


FIGURE 7 Primary sources of noise in the adhesive bond inspection problem.

Fourier Transform was used in the study as a data reduction technique since a 512 point amplitude-time signal could be represented by 50 frequency components in a Fourier Transform spectrum. Thus a significantly reduced feature vector was able to represent the signal in the frequency domain. Furthermore, the ultrasonic signal could then be described by only a few characteristic features such as peak frequency, 6 dB down bandwidth, and number of significant depressions. These features were then used in a pattern recognition algorithm to classify the ultrasonic signal's origin.

FEATURE SELECTION

One of the more critical steps in the implementation of any pattern recognition technique is the selection of the best features to distinguish the different classes being studied. To aid in feature selection, a theoretical computer-generated model, based on Brekhovskikh's layered media theory,¹² was developed to provide a large set of idealized ultrasonic transfer function data for a variety of adhesive bonding situations. These transfer functions, examples of which are displayed in Figure 8, provided a means to select the distinguishing features. In the example described by Figure 8, two of the discriminating features would be depression depths and areas under the curve for various frequency intervals. Features from the theoretical study were then compared with the same features from the actual bond specimens to determine their usefulness. Features found promising by other authors^{2,3,6,13,14} were also considered and either incorporated into the algorithm or rejected. The features used (see Table III) and their physical significance were as follows:

- 1) The peak-to-peak ratio of the echo and the reference signal in the amplitude-time domain, as illustrated in Figure 9, was representative of the reflection coefficient at the adherent-adhesive interface due to the acoustic impedance mismatch. A large ratio would indicate such flaws as surface

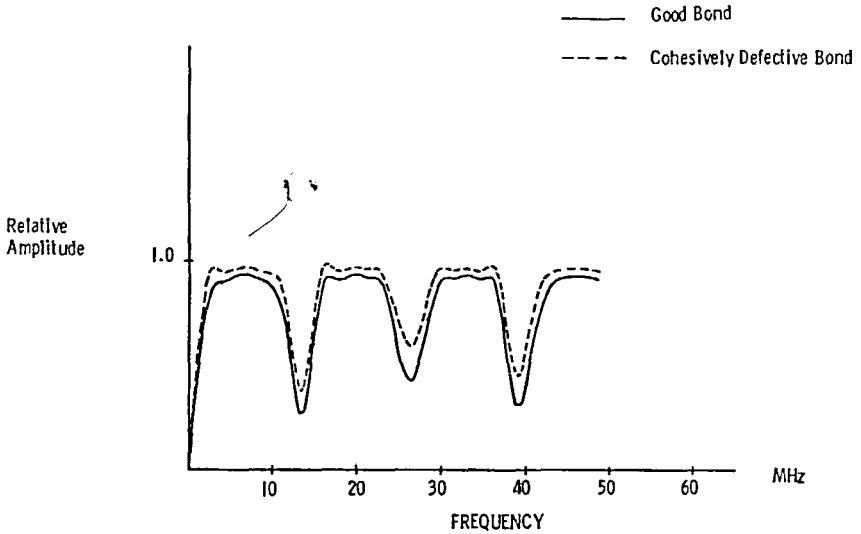


FIGURE 8 Example of good bond's and cohesively poor bond's transfer functions - theoretical derived.

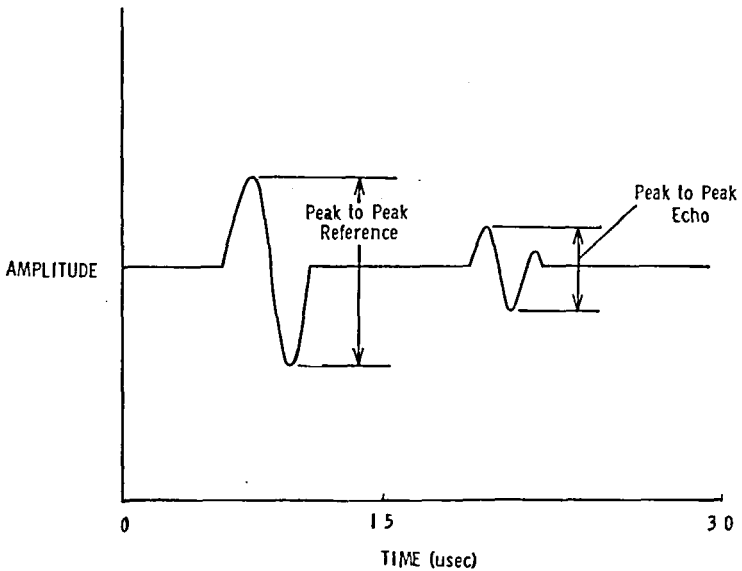


FIGURE 9 Typical ultrasonic signal reflected from bond specimen, displaying reference and bond layer echoes.

input pulse where the interface echoes could be separated in the time domain. Such a transducer was not available at the time of this study.

2) Frequency shift, as illustrated in Figure 11, from the reference signal's Fourier spectrum peak frequency to echo signal's Fourier spectrum peak frequency was caused by attenuation effects of the bond layer. Attenuation has been related to bond integrity by several investigators.^{2,15}

3) Peak frequency of the transfer function was compared with the reference peak frequency (see Figure 12) to detect the extent of frequency shifting caused by bond layer attenuation and destructive interference. Attenuation, as shown in references^{2,5,14,16} is an indicator of the state of adhesive cure and the cohesive bond strength.

4) Dip frequency, or frequencies, was also measured from the transfer function (see Figure 12) and is related to the adhesive layer's thickness and the velocity of sound in the adhesive. The bond layer thickness can be calculated from the equation $t = (\text{velocity in bond layer}) / (2 \text{ times dip frequency interval})$, assuming the sound velocity is known. Likewise, the dip frequency spacing is indicative of the velocity of sound in the adhesive bond layer. Adhesive bond sound velocity has been related to the cure state of the bond^{14,16} which effects the cohesive strength.

5) The dip amplitude divided by peak amplitude of the transfer function is related to the destructive interference at the half-wavelength thickness of the bond layer. The depth of the dip is related to the degree of destructive

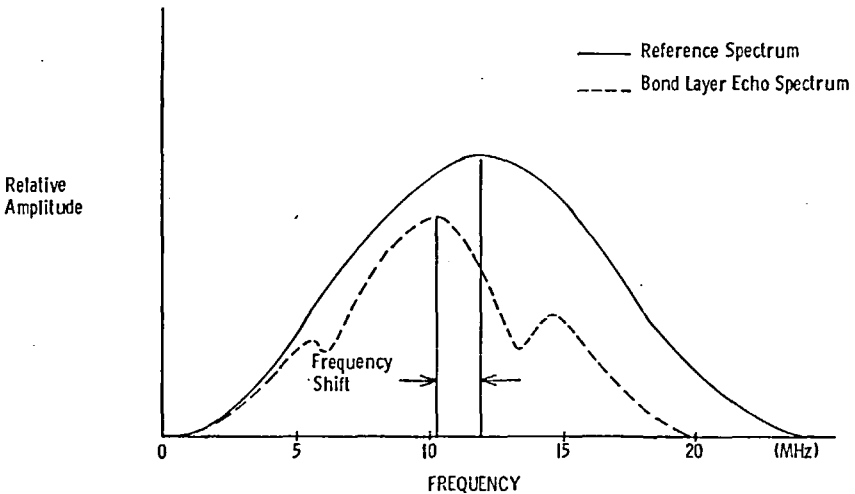


FIGURE 11 Feature selection from Fourier spectrum domain.

- A - Peak Frequency
- B - Dip Frequency
- C - Dip - Peak Frequency
- D - Dip/Peak Amplitude
- E - DP2 - DPI Frequency
- F - 6 db Down Bandwidth

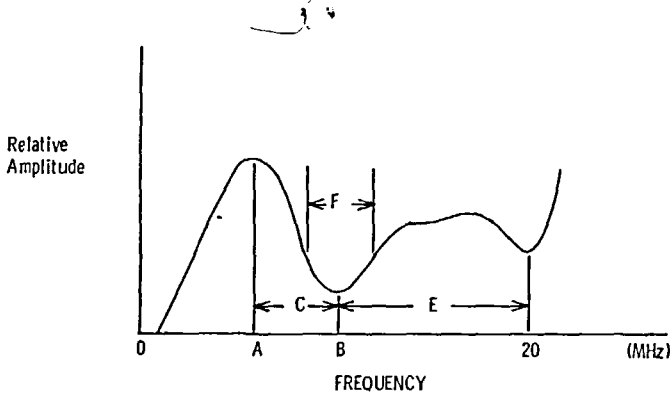


FIGURE 12 Features selected from transfer function.

interference. As the bond layer's attenuation increases, the degree of interference is decreased and the dip depth is lessened. Attenuation has been compared with the state of cohesive strength of the bond.^{2,6,14,16}

6) Frequency separation between first and second depressions in the transfer function domain (see Figure 12) is related to the bond layer thickness and the wave speed in the adhesive by the equation:

$$\text{bond layer thickness} = \frac{\text{wave speed in adhesive}}{2 (\text{frequency separation})}$$

The bond layer thickness, if too large or too small, will cause a poor bond; or an undercured adhesive will have a slow wave speed and look like a thick bond layer.

7) Standard Deviation of the transfer function is a statistical feature which seemed to relate to the quality of the bond layer. This feature was discovered and tested during the theoretical, parametric study phase of this research effort and showed promise for aiding the classification.

8) The primary depression width at the halfway-down location (see Figure 12) is also related to the extent of destructive interference and has been investigated by Chang *et al.*¹³

ALGORITHM DEVELOPMENT

After the entire set of bond specimens had been ultrasonically inspected and the data stored in the computer, the bond defect prediction algorithm was developed. A fairly large set of specimens was used to produce an accurate bond defect prediction scheme. The data set, which in this study included 154 bonds, was Fourier Transformed and the transfer functions were calculated. The features as listed in Table III were gathered from the signals and their transfer functions. The advantage of using features from the transfer function as alluded to by Rose and Thomas⁸ was the transducer-independent nature of the transfer function. By selecting features in the transfer function domain the noise problems of deconvolution as described by Rose and Avioli⁹ were not involved. The data set of features were then separated into two random groups, the training set and the test set. The first set of 64 specimens (see Table I) was used in the Fisher Linear Discriminant⁸ function to calculate the optimal coefficients for the linear discriminant function. The same data was then substituted into the Fisher Linear Discriminant function's equation and the scalar result for each bond specimen calculated. These scalar results were then correlated with their respective failure loads and a threshold for the good bond-bad bond boundary derived. The final task was to test the second set of 90 unknown bond specimens (see Table II) with the linear discriminant function so as to determine the bond strength prediction algorithm's reliability. If the reliability was not acceptable, the process was restarted using improved data acquisition, better signal processing, and possibly different features.

RESULTS

Two sources of feature values were considered for this sample problem of adhesive defect prediction. First, a more classical technique of selecting features from the Fourier transform frequency spectrum was considered, but this method was dependent on the transducer as described by Rose and Thomas.⁸ Their method used Fourier spectrum features in a Fisher Linear Discriminant function to classify adhesively defective bond specimens and was 91% reliable for the design transducer (see Table IV). Any other transducer produced poorer results. Table IV also presents the results from an earlier study conducted by Rose and Thomas⁸ to predict "adhesive defects" in aluminum-to-aluminum, step-lap specimens. This study differed from the present study because the present study includes cohesive defects as well as adhesive defects. A second, more desirable, technique of directly selecting

TABLE IV

Sample problem results compared with results of previous adhesive bond study

	Training set		Test set	
	Reliability	Loss function	Reliability	Loss function
Rose and Thomas Fisher algorithm (adhesive defect only)	96%	100%	88%	100%
Fisher algorithm using Fourier spectrum features	97%	100%	74%	87%
Fisher algorithm using transfer function features	91%	97%	84%	91%

most of the features from the transfer function of the bond system was considered because of its inherent transducer independence. Both methods of selecting features used the same training set and test set of specimens. Both methods considered a two class problem: good or bad bonds. The bad bonds in this study had either adhesive defects or cohesive defects. The adhesive defects were caused by surface contamination as in the earlier study⁸ and the cohesive defects were manufactured by undercuring the adhesive. Features from the earlier study⁸ were used to find adhesive problems and new features, determined by a theoretical study, were added to find the cohesive problems.

The first method of selecting features from the Fourier transform provided rather reliable results, but again these results were only good for a single transducer. The training set of specimens' defects were predicted with 97% reliability by the Fourier transform alone. The test set reliability dropped to 74% when using only the Fourier transforms for feature value determination, Table IV. In this case, as in the second case, a Fisher Linear Discriminant function was designed to predict the adhesive bond defects.

The second method, using the transfer function, provided a 91% reliability for the same 64 bond specimens used in the previous training set. The algorithm was designed to produce an optimal loss function reliability, which in this case was 97%. The total reliability of an adhesive bond defect prediction algorithm was defined as the percentage of correct predictions compared to the total number of predictions. However, the loss function reliability of the algorithm was defined as the percentage of correct predictions, where calling a good bond bad was considered a correct prediction, compared to

the total number of predictions. Thus, the loss function analysis concept allows for the incorrect prediction of good bonds, but does not tolerate incorrect prediction of defective bonds. Sometimes adjusting the pattern recognition algorithm to produce best loss function results decreased the total reliability of the algorithm. A test set of 90 bond specimens was inspected and the transfer function-based algorithm provided an 84% reliability, which was better than the Fourier transform based algorithm for the same specimens, see Table IV. Also, the loss function results for this test set, using the transfer function approach, was 91% reliable.

Though loss function analysis is an important concept, the results could be misleading. One could obtain a 100% reliability from the loss function approach by simply classifying all bonds as bad. A way to describe the results in an unbiased manner is discussed by Swets¹⁷ and is called Receiver Operating Characteristic (ROC) curves. To use this technique, one first plots the probability density curve of the scalar results from the Fisher Linear Discriminant equation for both classes, good bonds and poor bonds, see Figure 13a. In most classification problems, these classes have an overlap region that causes the incorrect predictions. It is this overlapping region that is being considered by the ROC curves. If a threshold boundary (c) is set, see Figure 13a, then the bonds are in one class if the scalar result (a) of the Linear Discriminant is less than c and the bonds are in the other class if a is greater than c . By shifting c from one class extreme to the other class extreme (a to b in Figure 13a), the probability of a correct prediction can be plotted versus the probability of a false alarm and this graph is the ROC curve, see Figure 13b. In this study a correct prediction is when a bad bond is classified as a bad bond. Figure 13b illustrates the benefit of the ROC curve by a comparison of three curves. The top curve is the ROC plot for the results of the Fisher Linear Discriminant function using features from the transfer function domain and shows the greatest probability of a hit for a certain probability of a false alarm of all the curves. The middle curve is the results of the Fisher

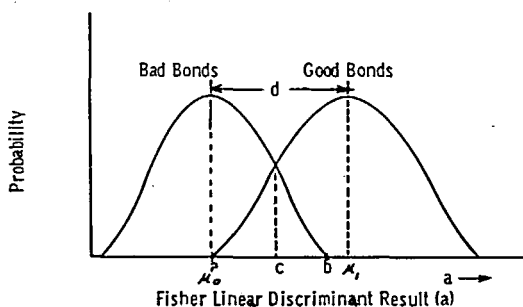


FIGURE 13a Probability density curve.

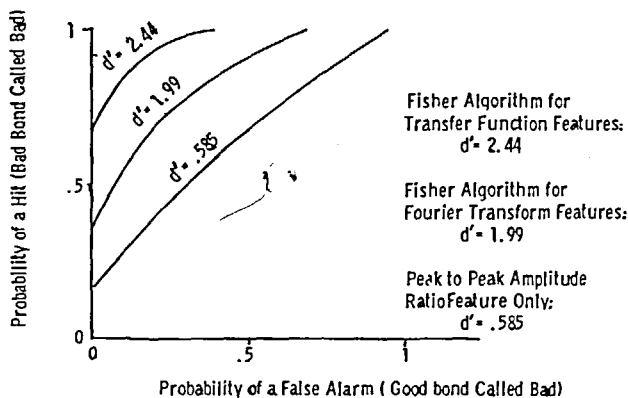


FIGURE 13b Receiver operating characteristic curve for three classification techniques.

Linear Discriminant function only. In this case the features were extracted from the Fourier spectrums and this curve indicates a lesser probability of a hit for the same probability of a false alarm. Finally, the bottom curve was derived from the results of the classification scheme using only the peak-to-peak amplitude ratio feature and the ROC curve illustrates that this method was the worst of the three. These curves are parameterized by a value d' . The parameter d' is the difference between the means of the probability density curves ($H_1 - H_0$), see Figure 13a, divided by the standard deviation of the curve representing the bad class. In summary, the ROC technique provides an impartial means for determining the relative merit of various classification methods.

CONCLUSIONS

A major concern of the adhesive bonding industry has been the nondestructive evaluation of the bond layer in an assembled structure. This study has produced a computer augmented, ultrasonic test bed system which was designed to attack and solve problems in classifying adhesive bonding defects. The types of problems considered were not the gross flaws such as delaminations or debonds but the more subtle defects such as improper surface preparation and adhesive undercure. State of the art ultrasonic data acquisition procedures, sophisticated signal processing and feature extraction methods, and advanced pattern recognition techniques were incorporated in the test bed system.

A sample problem of identifying improper surface preparation or adhesive undercure in aluminum-to-aluminum step-lap joints has been solved using

the ultrasonic test bed system. An overall reliability of 91% has been achieved for this classification problem. The success of this sample problem clearly indicates the potential of the ultrasonic test bed to solve many of the adhesive bonding inspection problems plaguing the industry today.

References

1. J. W. Raisch and J. L. Rose, *Materials Evaluation* 37, 55-64 (1979).
2. Paul L. Flynn, "Cohesive Strength Prediction of Adhesive Joints," *Proceedings of the ARPA/AFML Review of Progress in Quantitative Nondestructive Evaluation*, Technical Report AFML-TR-77-44, pp. 59-65, January 1977.
3. F. H. Chang, R. A. Kline and J. R. Bell, "Ultrasonic Evaluation of Adhesive Bond Strength Using Spectroscopy Techniques," presented at ARPA/AFML Conference in La Jolla, California, July 1978.
4. J. C. Couchman, B. G. W. Yee and F. H. Chang, *Materials Evaluation* 37, 48-50 (1979).
5. G. A. Alers, *et al.*, "Ultrasonic Measurement of Interfacial Properties in Completed Adhesive Bonds," presented at the ARPA/AFML Conference in La Jolla, California, July 1978.
6. G. A. Alers and R. K. Elsley, "Ultrasonic Measurement of Adhesive Bond Strength," Rockwell Science Center Report No. SC595.32SA, Project III, Unit A, Task I.
7. A. N. Mucciardi and R. K. Elsley, "Characterization of Defects in Adhesive Bonds by Adaptive Learning Networks," presented at the ARPA/AFML Conference in La Jolla, California, July 1978.
8. J. L. Rose and G. H. Thomas, *British Journal of NDT* 21, 135-139 (1979).
9. J. L. Rose and M. J. Avioli, "Transducer Compensation Concepts of Value in Flaw Classification," presented at the Spring ASNT Conference, New Orleans, 1978, and to be published in a reliability supplement to *Materials Evaluation*.
10. J. L. Rose and M. J. Avioli, "Generalized Approach to New Problems in Ultrasonic Inspection," Naval Air Engineering Center report, February 12, 1979.
11. F. Erdogen and M. Ratwani, *J. Composite Materials* 5, 378 (1971).
12. L. M. Brekhovskikh, *Waves in Layered Media* (Academic Press, New York, 1960).
13. F. H. Chang, *IEEE Transactions on Sonics and Ultrasonics*, SU-23, 334-338 (1976).
14. P. L. Flynn and S. P. Henslee, "Cohesive Bond Strength Prediction," Rockwell Science Center Report No. SC595.32SA, Project III, Unit A, Task 3.
15. P. A. Meyer and J. L. Rose, *J. Applied Physics* 48, 3705-3712 (1977).
16. A. M. Lindrose, *Experimental Mechanics* 18, 227-232 (1978).
17. J. A. Swets, *Science* 182, 990 (1973).